



Semnan University

Mechanics of Advanced Composite Structures

journal homepage: <https://MACS.journals.semnan.ac.ir>

Influence of Filler Content on the Mechanical, Thermal, Moisture Absorption, and Biodegradability Properties of Bionanocomposite with Cellulosic Fibers Derived from Delonix Regia Fruits

K. P. Kaurase*^{ORCID}, D. Singh^{ORCID}

School of Aeronautical Sciences, Hindustan Institute of Technology and Sciences, Hindustan University, Chennai, India

KEYWORDS

Bionanocomposite;
Delonixregia fruit fibers;
Mechano-chemical treatment;
SEM;
Mechanical test;
Biodegradability.

ABSTRACT

Cellulose is one of the most widely used and widely available materials on the planet, and it has been used for centuries in a wide range of applications. In this paper, a new source of cellulose delonix regia fruits has been explored for the extraction of cellulose at the micro and nanoscale. Cellulose is isolated from the raw delonix regia fruits by sub-sequential chemical methods such as pulping, bleaching, delignification, and acid hydrolysis. PVA/CMF and PVA/CNF composites are prepared by the solvent casting process with 1, 3, 5, 7, and 9 percentages of filler concentration. Mechanical, thermal, morphological, moisture absorption, and biodegradability properties of pure PVA, PVA/CMF, and PVA/CNF composite at different filler concentrations were evaluated using mechanical testing (tensile, flexural, and impact), TGA-DTG, SEM, moisture absorption test and soil burial test respectively. The SEM results showed that at increased filler content concentrations, signs of agglomeration began to occur, and the overall performance of the resulting composite material degraded due to which filler addition should be limited to less than 7wt%. Tensile, flexural, and impact test results revealed that nano-fillers performed better than micro-fillers, and the best performance is obtained with filler content below 7%. The degradation temperature of composites with filler content improved dramatically, according to TGA and DTG curves, and composites with nano-fillers had greater thermal stability than composites with micro-fillers. The inclusion of filler content reduced the tendency of composite materials to absorb moisture and the resulting composite materials had enough biodegradation rate together with higher lifetime and performance, according to the findings of the biodegradability test and moisture absorption test.

1. Introduction

In the last few decades, synthetic polymers and their derivatives have seen significant application and it has reached every household due to their flexibility to mold in any shape and size, easy availability, lightweight, high specific strength, and durability. These materials are basically petroleum derivatives which are fossil fuels and the major issue with these materials is their non-renewability. Another major concern related to these materials is that the resources of fossil fuels are depleting day by day which encouraged most of the researchers all over the world to search for alternatives [1, 2]. Also, these

materials do not degrade easily over a long period of time and hence create landfills. Due to all these reasons researchers have started exploring new biodegradable alternatives to synthetic polymers which can provide sustainable solutions to the problem of increasing landfills. Biopolymers are generally categorized as natural biopolymers, synthetic biopolymers, and microbial biopolymers. Some of the commonly used biopolymers are polypeptides, nucleic acids, collagen, natural rubber, lignin, cutin, sugars, gelatin, starch, cellulose, alginate, chitosan, polylactic acid, Polyvinyl alcohol, etc. However, these biopolymers

* Corresponding author. Tel.: +91-7509949676
E-mail address: kalpitkaurase@gmail.com

lack mechanical properties which impose serious limitations on their widespread application. These biopolymers can be reinforced with various compatible natural fibers at the macro, micro, and nano-scale to improve the mechanical properties of the composite. Polyvinyl alcohol (PVOH/PVA) is prepared by saponification of polyvinyl acetate and is a water-soluble synthetic biopolymer. It is a colorless and odorless chemical with the formula $[\text{CH}_2\text{CH}(\text{OH})]_n$ and is widely used as a thickener and emulsion stabilizer in different industries like carpentry, paper, textile, and specifically in the medical industry due to its biocompatibility with most of the biomaterials [3-5].

Cellulose derived from lignocellulosic biomasses is one of the most suitable choices for preparing biocomposite materials with these biopolymers. The use of lignocellulosic biomasses is not new to mankind; it has been used over the centuries for a variety of applications such as animal fodder, building houses, paper making, etc [6-7]. Lignocellulosic biomass can be obtained from different sources including plants, animals, agricultural wastes, urban wastes, etc., and differ in the concentrations of contents. The major contents of these biomasses are cellulose, hemicelluloses, lignin, pectin, wax, protein, starch, fat, ash, and other residuals [8-9]. Quantitatively the amount of contents differs for the same source depending on geological location and growing conditions. Cellulose is the most important constituent of the plant structure which is entrenched in lignin and provides structural strength to the entire plant. Cellulose can be obtained in the form of fibers, particles, or crystals at macro, micro, and nano-scales. Cellulose can be obtained by top-down or bottom-up approaches; some of the most frequently used top-down approaches are acid hydrolysis, bleaching, enzymatic hydrolysis, tempo oxidation, and pulping which are termed chemical methods. Mechanical methods like ultrasonication, high-energy ball milling, and high-pressure homogenization can also be used for isolating cellulose along with chemical methods. Smaller particle size of nano cellulose offers improved surface area which results in better wettability with polymers and hence significant increment in mechanical, thermal, and other properties [10-11]. Based on structure and morphology nano cellulose can be categorized as cellulose nanofibers (CNF), cellulose nanocrystals (CNC), and cellulose nanowhiskers (CNW).

Delonix regia (Gulmohar) fruits were selected as a novel source for cellulosic nanofibers (CNF) due to their high percentage of cellulose [6]. Also, another reason for the selection of Delonix Regia (Gulmohar) fruits is its wide availability and non-

utilization for any kind of application. Mechanochemical methods are used for extracting cellulose at the nanoscale and further biocomposite material was prepared with polyvinyl alcohol by using the solvent casting method. The main aim of the research is to analyze the effect of filler content on the morphological, mechanical, thermal, optical, water absorption, and biodegradable properties of the prepared bio-nanocomposite material and to validate its area of application.

2. Experimental Procedures

2.1. Isolation of Cellulosic Nano-Fiber (CNF)

All the chemicals used in the isolation process were of analytical grades and obtained from Navakar Chemicals, Chennai. Raw delonix regia fruits (DRF) were collected from the local fields of Nagpur. Before being subjected to chemical treatments, the seeds of DRF fruits were removed and the size of fibers was reduced by chopping and grounding.

Micro and nano-cellulose used in this work were isolated from delonix regia fruit fibers by mechanochemical treatments as per the procedure mentioned in earlier work [6, 9, 10].

Initially, Soxhlet extractive removal procedure was applied to 20 g of delonix regia fruit fiber samples. The round flask was filled with 2:1 (v/v) toluene/ethanol mixture and the heating mantle was turned on for 6 hours at 90°C before washing with ethanol and drying. To improve the fiber swelling and to remove the lignin and hemicellulose partially, fibers were chemically pulped with 17.5% (w/w) Sodium Hydroxide (NaOH) at room temperature for 24 hrs followed by cleaning and filtration.

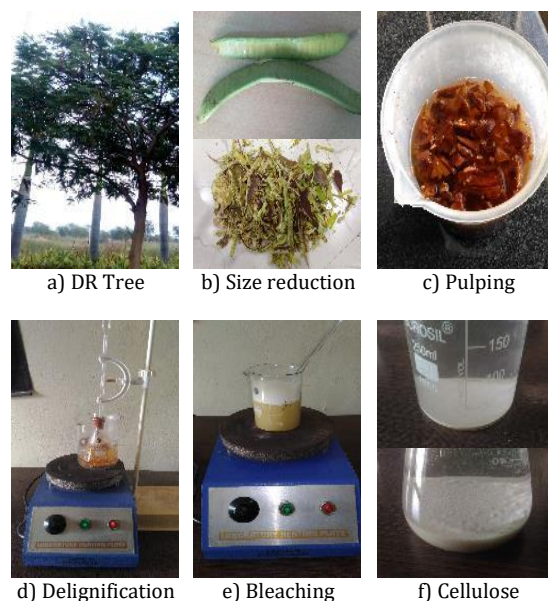


Fig. 1. Cellulose isolation procedure

Fibers were delignified by treating them with 72% (v/v) sulfuric acid (H_2SO_4) at 70°C for 1 hour and centrifuged to achieve a neutral pH. To get rid of hemicellulose, fibers were given a mild alkaline treatment with 2% (w/w) NaOH at 90°C for 2 hrs in a water bath. Further, fibers were repeatedly rinsed and filtered after being bleached five times with 5% (v/v) sodium hypochlorite at 75°C for 2 hrs. To obtain highly purified cellulose, fibers were finally bleached with 10% (v/v) hydrogen peroxide (H_2O_2) at 80°C for 1 hr. The filtrate was then oven-dried at 40°C for 5 hrs [9, 10]. Figure 1 depicts the cellulose isolation procedure.

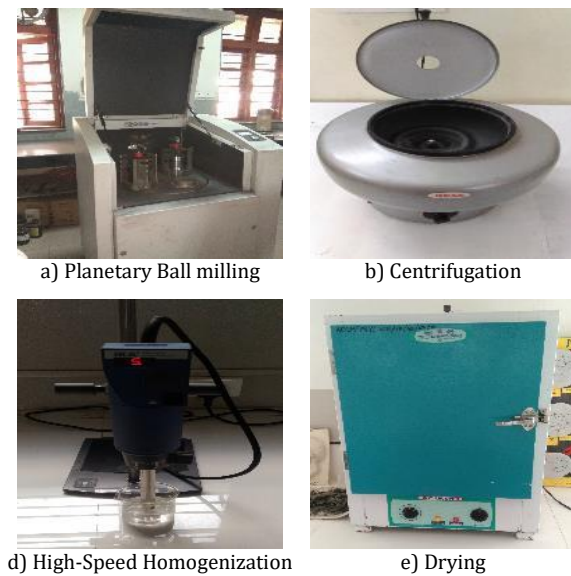


Fig. 2. Cellulosic Nano Fibers (CNF) isolation process

A high-energy planetary ball mill machine PM 400 Retsch, Germany with a tungsten carbide jar was used to mechanically reduce the size of the cellulose fibers. The jar was filled with 1/3rd volume of dried cellulose and 10 mm diameter tungsten carbide balls in the ratio of 60:1 (%wt) were rotated at 600 rpm for 1 hr and sieved through 200 mesh to obtain nano-sized cellulose. Further, the fibers were treated with 5% ethanol and centrifuged with deionized water at 5000 rpm for 5 minutes. The samples were then combined with deionized water and homogenized for 2 minutes at 15000 rpm using an Ultra-Turrax T-25 high-speed homogenizer (IKA, Germany). The homogenized samples were dried at 80°C for 4 hrs to remove water and stored in a desiccator for further use [10, 12]. Figure 2 shows the cellulosic Nano fibers isolation process.

2.2. Preparation of Bionanocomposite

Bionanocomposite was prepared by solvent casting technique with Poly Vinyl Alcohol (PVA) and cellulosic nanofibers (CNF). For producing a homogeneous polymeric solution, 10 wt% of PVA

granules were dissolved in distilled water and the temperature was gradually raised from 35°C to 80°C with continuous magnetic stirring at 700 rpm for 1 hr.

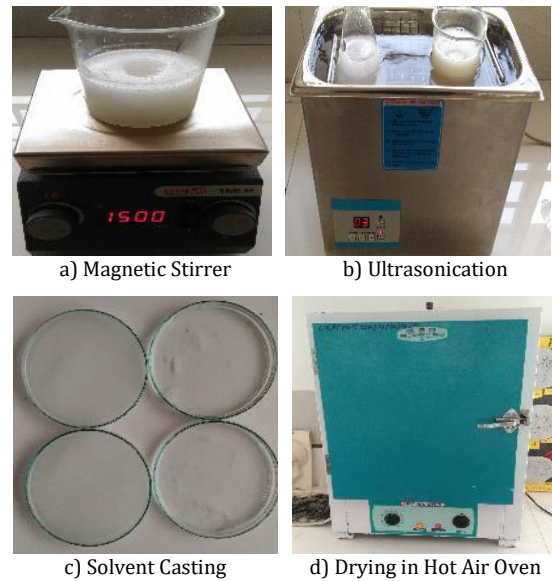


Fig. 3. PVA/CMF & PVA/CNF Composite preparation procedure

After 1 hr of mixing, 5 wt% of glycerol (GL) was added as a plasticizer and the polymeric solution was vigorously stirred for 30 minutes. 1, 3, 5, 7, and 9 wt% of Cellulosic Micro fibers (CMF) and CNF were added to the polymeric solution with continuous magnetic stirring at 1500 rpm for 2 hrs to produce a PVA/CMF and PVA/CNF composite.

The solution was ultrasonicated for 10-20 minutes to avoid agglomeration. Homogenous composite solutions were put in petri dishes to gently evaporate the solvent for 2 hrs before the mixture was dried for 3 hrs in a hot air oven.

Obtained pure PVA, PVA/CMF and PVA/CNF composite films were labeled as PVA, PVA/CMF1, PVA/CMF3, PVA/CMF5, PVA/CMF7, PVA/CMF9, PVA/CNF1, PVA/CNF3, PVA/CNF5, PVA/CNF7 and PVA/CNF9 and stored in a desiccator for further use [12-15].

2.3. Scanning Electron Microscopy

Scanning electron microscopy (SEM) was performed at 18 kV on the PVA, PVA/CMF, and PVA/CNF specimens to understand the morphological properties of the bionanocomposite. Before performing imaging the samples were coated with gold [16-18].

2.4. Mechanical Properties

• Tensile Test:

To understand the effect of filler addition on the mechanical properties of prepared

bionanocomposites, tensile tests were conducted on PVA, PVA/CMF, and PVA/CNF composite specimens using a Universal Testing Machine (TKG-EC 500 N) at room temperature with 10 mm/min speed and 25 mm grip spacing. All the tests were performed according to ASTM D 882-92 standards. The uniform dimension of 25 mm × 3 mm was maintained for all the test specimens and every test was performed thrice to confirm the repeatability. All the samples were conditioned at room temperature and relative humidity of 50% before being subjected to mechanical testing. Tensile strength (σ_{\max}) and percentage elongation (%EL) were obtained using the following equations:

$$(\sigma_T)_{\max} = \frac{P_{\max}}{A_{cs}} \text{ and } \%EL = \frac{L_f - L_0}{L_0} \times 100 \quad (1)$$

where

P_{\max} = Maximum Applied Breaking Load (N),
 A_{cs} = cross-sectional area of the material (mm²),
 L_f = Final Length at Breaking (mm),
 L_0 = Initial Length (mm).

- *Flexural Test:*

Three-point bending test was performed on PVA, PVA/CMF, and PVA/CNF composite specimens using the Universal Testing Machine (TKG-EC 500 N) at room temperature with a speed of 10 mm/min, as per ASTM D790 standards [19, 20]. All the specimens had dimensions of 80 mm × 15 mm × 3.5 mm. Every test was performed thrice to assure the repeatability and results were averaged. Flexural strength and flexural modulus are computed using the following equations:

$$(\sigma_{Fl})_{\max} = \frac{3P_{\max}x}{2wt^2} \text{ and } E_{fl} = \frac{mx^3}{4wt^3} \quad (2)$$

where

P_{\max} = Maximum Applied (N),
 x = Length of span (mm),
 w = Width of Specimen (mm),
 t = Thickness of Specimen (mm).

- *Impact Test:*

I-Zod impact test was conducted on PVA, PVA/CMF, and PVA/CNF composite specimens with an impact testing machine (Model: TM-IT-30) as per ASTM D 256 standards. All the specimens had dimensions of 65 mm × 12.7 mm × 12.7 mm with a notch thickness of 2.5 mm. Each test was conducted thrice to confirm the reproducibility and results were averaged [21, 22].

2.5. Thermal Properties

Thermal properties of PVA, PVA/CMF, and PVA/CNF composite films were obtained by

performing Thermo-Gravimetric Analysis (TGA) and Derivative Thermo-Gravimetric (DTG) Analysis with TA instruments (USA) SDT 2960. 10 mg sample was placed in an aluminum crucible and heated to temperatures between 30 and 750°C in a nitrogen environment by maintaining the flow rate of 80 ml per minute and heating rate of 10.00 K per minute. Change in mass of samples was measured using a microbalance device [23, 24].

2.6. Biodegradability Test

The biodegradability of PVA, PVA/CMF, and PVA/CNF samples was obtained by performing a soil burial test. A computerized weighing balance was used to determine the initial weight (W_i) after all samples were cut into 3 cm × 3 cm. These samples were kept at room temperature after being buried 10 cm deep in a closed plastic container. Water was regularly sprayed in the container to maintain a relative humidity (RH) range of 40 to 50% throughout the test. Over the total test duration of 20 weeks, the samples were examined within every two weeks [25-27]. After the test period, samples were cleaned with distilled water and dried for 24 hours at 70°C in a hot air oven, and their final weight (W_f) was determined using a digital weighing balance. Three samples of each material were evaluated to ensure the test process's reproducibility. The biodegradation rate was calculated using the following equation:

$$BDR(\%) = \frac{W_i - W_f}{W_i} \times 100\% \quad (3)$$

where

BDR = Biodegradation rate,
 W_i = Initial weight of the sample,
 W_f = Final weight of the sample.

2.7. Moisture Absorption Test

The moisture absorption rate of the PVA, PVA/CMF, and PVA/CNF specimens was evaluated using a moisture absorption test. The initial weight (W_i) of each sample was determined using a digital weighing balance after cutting the samples to 1 cm × 1 cm and drying them for 48 hours in a hot air oven at 60°C. These samples were kept in a closed chamber at room temperature and 75% relative humidity during the test (RH). Throughout the 6-hour test period, samples were examined every 30 minutes and weighed (W_f) each time using a digital weighing balance. Three samples of each material were evaluated to ensure the test process's reproducibility [28-30]. The moisture absorption rate was calculated using the following equation:

$$MAR(\%) = \frac{W_i - W_f}{W_i} \times 100\% \quad (4)$$

where

MAR = Moisture absorption rate,

W_i = Initial weight of the sample,

W_f = Final weight of the sample.

2.8. Particle Size and Zeta Potential Measurement

The isolated CMF and CNF were subjected to particle size and zeta potential measurements using the Nano Partica, Nano Particle Analyzer, SZ-100, Horiba Scientific, Japan. CMF and CNF samples were added to the quartz cuvette after diluting with distilled water. The measurement range was kept between 0.1 nm to 10000 nm and performed at room temperature (25°C). With a dispersion medium viscosity of 0.895 mPa.s and a count rate of 281 KCPS, the scattering angle was maintained constant at 900. Zeta potential was determined with electrode voltage of 3.4 V, dispersion medium viscosity of 0.897 mPa.s, the conductivity of 0.107 mS/cm keeping the temperature of the holder at 24.9°C [10, 31, and 32].

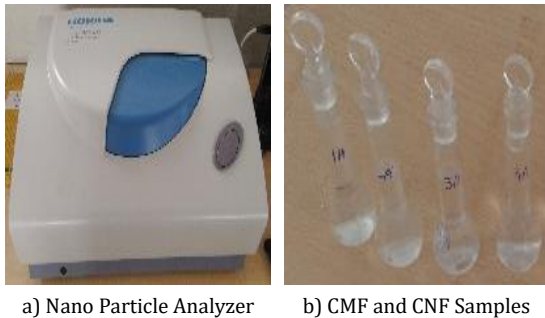


Fig. 4. Nano particle analyzer and CMF, CNF samples

3. Result and Discussion

3.1. Chemical Composition

The chemical composition of the Delonix Regia fruit fibers was obtained as per the previous work [6, 9, and 10]. Figure 5 illustrates the chemical composition of DRF fibers. Cellulose and hemicellulose content was estimated to be 66.9% and 11.6% respectively which is far better than the most popular cellulose sources like jute, kenaf, rice straw, wheat straw, corn, sugarcane baggase, etc [6]. This higher concentration of cellulose content makes the material cost-effective and a viable alternative for cellulose extraction.

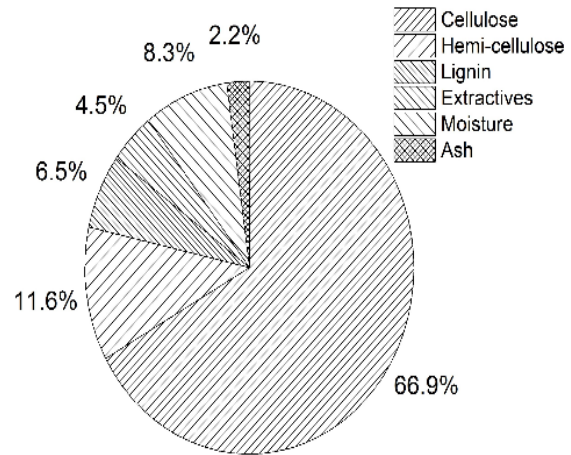


Fig. 5. Chemical composition of delonix regia fruit fiber (%w/w)

3.2. Scanning Electron Microscopy (SEM)

SEM micrographs of PVA, PVA/CMF, and PVA/CNF at 1, 3, 5, 7, and 9% of filler contents were shown in Figures 6 and 7. Smooth surfaces and consistent distribution of filler with no signs of cracking were observed for both PVA/CMF and PVA/CNF films with 1, 3, and 5% filler. Signs of agglomeration initiated as filler concentration reached 7% and it became significant at 9%.

From the micrographs, it was evident that at relatively greater filler concentrations, interactions between particles occur rather than interactions between filler and matrix which might degrade the properties of bionanocomposite. In order to achieve a uniform distribution of fillers in the PVA matrix without agglomerations and cracking, the concentration of fillers should be restricted below 7% [33-36].

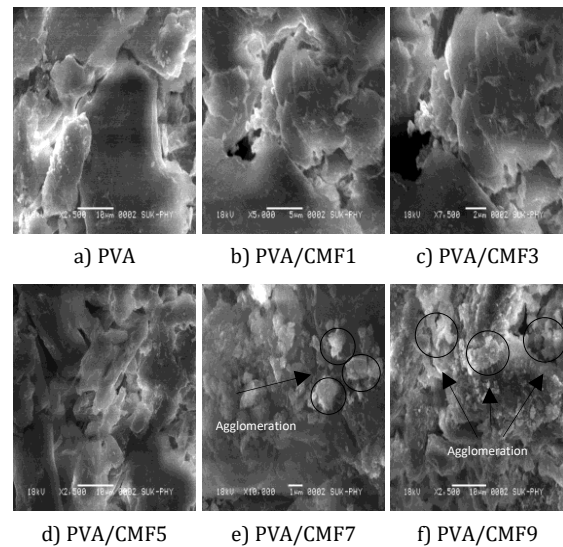


Fig. 6. SEM images of PVA/CMF samples

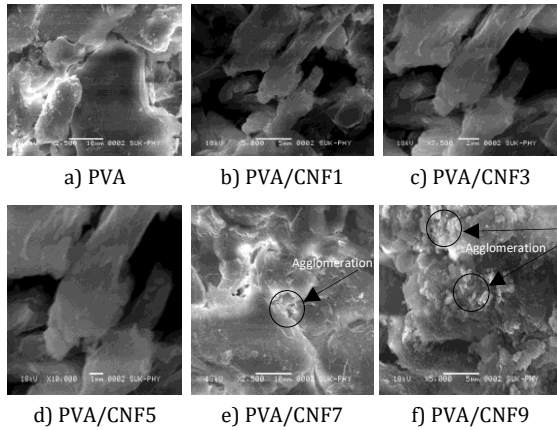


Fig. 7. SEM images of PVA/CNF samples

3.3. Mechanical Properties

a) Tensile Test

Tensile tests were used to assess the tensile modulus and percentage of elongation at the break of pure PVA, PVA/CMF, and PVA/CNF composite specimens at filler contents of 1, 3, 5, 7, and 9. Figure 8 shows the effect of variation of filler concentration on the tensile strength and percentage elongation of pure PVA, PVA/CMF, and PVA/CNF composite. The tensile strength of the pure PVA specimen was determined to be 46.2 MPa and a gradual increase in tensile strength was observed with increasing filler loading in both PVA/CMF and PVA/CNF composite specimens.

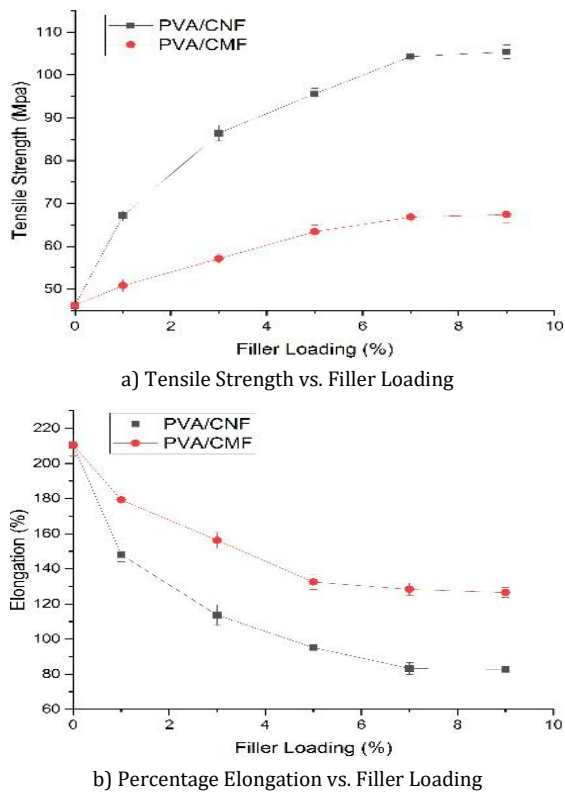


Fig. 8. Tensile Strength and Percentage Elongation of Pure PVA, PVA/CMF, and PVA/CNF Composite

The tensile strength was observed to increase by 32.09%, 51.31%, 50.79%, 56.14%, and 56.38% at 1, 3, 5, 7, and 9% filler content respectively for CNF as compared to CMF. There was an increment of 45.24% in tensile strength with a 1% addition of nano-filler, whereas tensile strength improved by only 9.96% with a 1% addition of micro-filler. Similarly, with the addition of 3%, 5%, 7%, and 9% nano-filler tensile strength improved by 87.01%, 106.93%, 125.76%, and 128.14% respectively, whereas with the addition of 3%, 5%, 7% and 9% micro-filler tensile strength improved by 23.59%, 37.23%, 44.59%, and 45.89% respectively. This increment was evident as the available surface area for bonding between filler and matrix is more for nano-fillers in comparison to micro-fillers.

A pure PVA specimen was found to have a percentage elongation of 210.5% and it was revealed that the percentage elongation decreased as the amount of filler was increased. As compared to micro-fillers, percentage elongation decreased by 17.40%, 27.27%, 28.23%, 35.15%, and 34.62% at 1, 3, 5, 7, and 9% nano-filler content respectively. With the addition of 1, 3, 5, 7, and 9% nano-filler percentage elongation decreased by 29.64%, 46.03%, 54.82%, 60.48%, and 60.71% respectively, whereas with the addition of 1, 3, 5, 7 and 9% micro-filler percentage elongation decreased by 14.82%, 25.8%, 37.05%, 39.05%, and 39.9% respectively. Significant improvement in tensile strength was seen upto 5% filler content, but the rate of increment in tensile strength slowed down after 5% filler content. A similar trend was observed for percentage elongation. A high amount of decrement in percentage elongation was seen up to the addition of 5% filler content, but very little decrement in percentage elongation was noticed for filler content above 5%. Hence, from the results obtained, it can be concluded that nano-fillers are more suitable for obtaining high-strength material, and filler content upto 5wt% gives the best performance of the bionanocomposite. The material composition should be determined by the needs of structural applications [37-39].

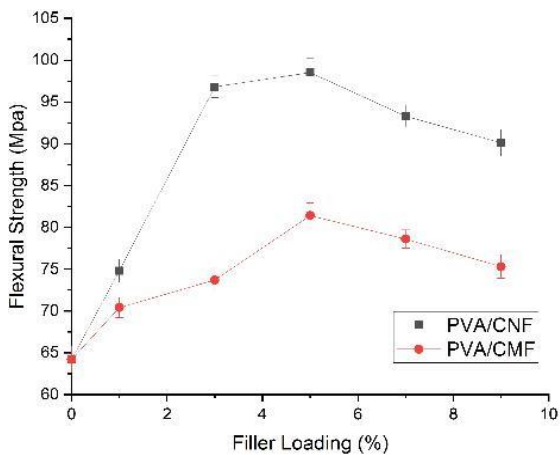
b) Flexural Test

Flexural strength and flexural modulus of pure PVA, PVA/CMF, and PVA/CNF composite specimens at nano-filler contents of 1, 3, 5, 7, and 9% were evaluated using the flexural test, and the results are depicted in Figure 9. Flexural strength and flexural modulus of a pure PVA specimen were observed to be 64.2 MPa and 2.34 GPa respectively. The value of flexural strength was observed to increase with upto 5wt% of filler

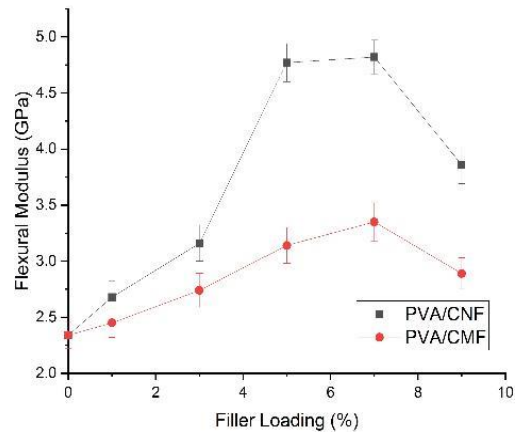
content and afterward, it started to decrease with further increment in filler content. A similar trend was observed for flexural modulus with an increment in the value upto 7wt% of filler content and further decrement with the addition of more filler.

Hence, from the analysis of the results of flexural strength and modulus, it can be concluded that the addition of nano-fillers is more suitable for obtaining high-strength material. Also, filler contents should be kept well below 5wt% to ensure quality products with excellent flexural strength and modulus. Flexural modulus was enhanced by 14.53%, 35.04%, 103.85%, 105.98% and 64.96% at 1, 3, 5, 7 and 9% nano-filler contents respectively, whereas it was enhanced by 4.7%, 17.09%, 34.19%, 43.16% and 23.5% at 1, 3, 5, 7 and 9% micro-filler contents as compared to flexural modulus of pure PVA specimen.

For both PVA/CMF and PVA/CNF composite, the value of flexural strength and flexural modulus was noticed to increase upto 5wt% of filler content and afterward rate of increment gradually decreased. Compared to the addition of micro-filler, flexural strength was enhanced by 6.25%, 31.34%, 21.01%, 18.7%, and 19.65% by the addition of 1, 3, 5, 7, and 9% nano-filler contents respectively. For PVA/CNF composite, flexural strength increased by 16.51%, 50.78%, 53.43%, 45.33% and 40.34% at 1, 3, 5, 7 and 9% nano-filler contents, whereas flexural strength was enhanced by 9.66%, 14.8%, 26.79%, 22.43% and 17.29% at 1, 3, 5, 7 and 9% micro-filler contents as compared to flexural strength of pure PVA specimen. In comparison to PVA/CMF, flexural modulus increased by 9.39%, 15.33%, 51.91%, 43.88%, and 33.56% by the addition of 1, 3, 5, 7, and 9% nano-filler contents respectively.



a) Flexural Strength vs. Filler Loading



b) Flexural Modulus vs. Filler Loading

Fig. 9. Flexural Strength and Modulus of Pure PVA, PVA/CMF, and PVA/CNF Composite

c) Impact Test

Impact strength of pure PVA, PVA/CMF, and PVA/CNF composite specimens at filler contents of 1, 3, 5, 7, and 9 and the results were shown in figure 10. The impact strength of a pure PVA specimen was estimated to be 12.63 KJ/mm² and it was seen that the value of impact strength increased as the amount of filler content increased upto 7% and afterward it started decreasing. The impact strength of the composite material with 1, 3, 5, 7, and 9wt% nano-filler improved by 15.42%, 15.84%, 13.24%, 16%, and 16.43% respectively as compared to the impact strength of composite with micro-filler content. In comparison to pure PVA specimen, the impact strength of PVA/CNF composite with 1, 3, 5, 7, and 9wt% filler enhanced by 30.96%, 45.37%, 59.78%, 68.8%, and 51.46% respectively. Similarly, when PVA/CMF composite impact strength was compared with pure PVA it was observed that at 1, 3, 5, 7, and 9wt% filler content impact strength improved by 13.46%, 25.49%, 41.09%, 45.53%, and 30.09% respectively. The obtained results indicated that composite material with nano-filler exhibited higher values of impact strength when compared with composite with micro-filler content due to the fact that nano-fillers have more exposed surface area for bonding with matrix which causes significant improvement in impact strength. Also, it was observed that the increment in impact strength was consistent upto the addition of 7wt% of nano and micro filler and further impact strength started decreasing. This trend suggests limiting the filler content to the maximum possible value of 7wt%.

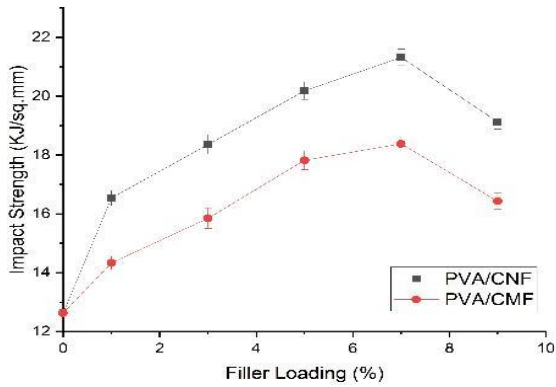


Fig. 10. Impact Strength of Pure PVA, PVA/CMF and PVA/CNF Composite

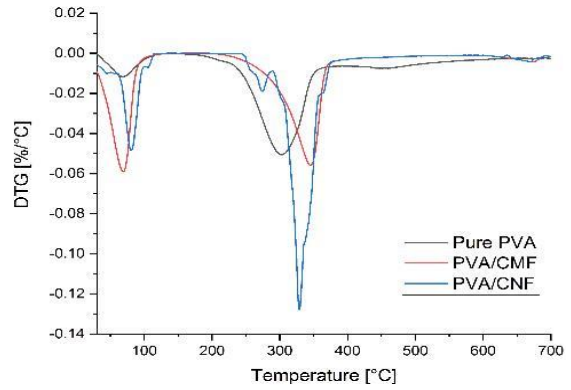


Fig. 12. DTG plots of pure PVA, PVA/CMF, and PVA/CNF composites

3.4. Thermal Properties

Thermal stability of PVA, PVA/CMF, and PVA/CNF composite specimens was determined by Thermo Gravimetric Analysis (TGA) and Derivative Thermo-Gravimetric (DTG) Analysis. Figure 11 shows the weight loss versus temperature curve of raw PVA, PVA/CMF, and PVA/CNF composite specimens, and Figure 12 shows the weight loss rate (derivative of weight loss) versus the temperature curve of the same material samples. The first degradation curve of PVA, PVA/CMF, and PVA/CNF was observed between 42.5°C to 105°C, 34°C to 98°C and 62.5°C to 103°C with almost 7.12%, 28.13%, and 13.99% weight loss respectively. The first degradation curve resulted from the evaporation of absorbed moisture during the initial heating of the sample.

The second degradation curve of PVA, PVA/CMF, and PVA/CNF occurred between 231.5°C to 344°C, 263.5°C to 372°C and 305.5°C to 358°C respectively, and continued till the material weight was reduced by almost 54.44%, 65.96%, and 65.89% respectively.

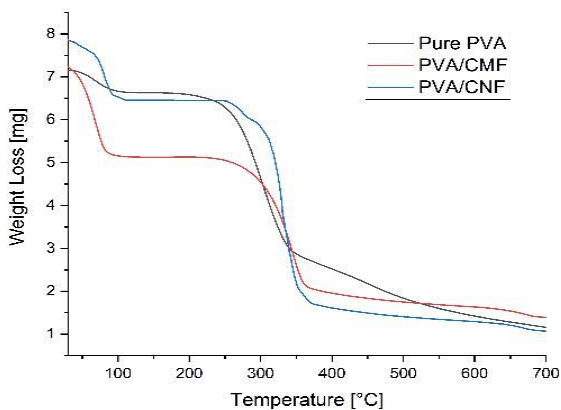


Fig. 11. TGA plots of pure PVA, PVA/CMF, and PVA/CNF composites

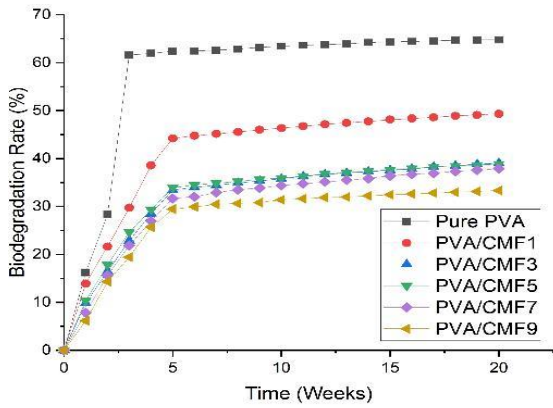
The second degradation curve shows the degradation of PVA's intermolecular hydrogen bonds, its dehydration reaction on the polymer chain, and the deterioration of its primary backbones over time.

Major weight loss of pure PVA was noticed at 301°C, whereas that of PVA/CMF and PVA/CNF samples occurred at 343.3°C and 329°C respectively. The third minor degradation region of PVA, PVA/CMF, and PVA/CNF was observed between 435°C to 479°C, 655°C to 687.5°C and 658°C to 690.4°C respectively with 16.28%, 8.26% and 7.44% weight reduction respectively. Third degradation represents carbonization of organic contents due to the ashing of the product. The results obtained indicated that the degradation temperature of PVA/CNF and PVA/CMF composite increased significantly compared to the pure PVA sample and the amount of material degraded also decreased for PVA/CMF and PVA/CNF composite. TGA results showed signs of improvement in the thermal stability of PVA/CMF and PVA/CNF samples compared to pure PVA samples [40-44].

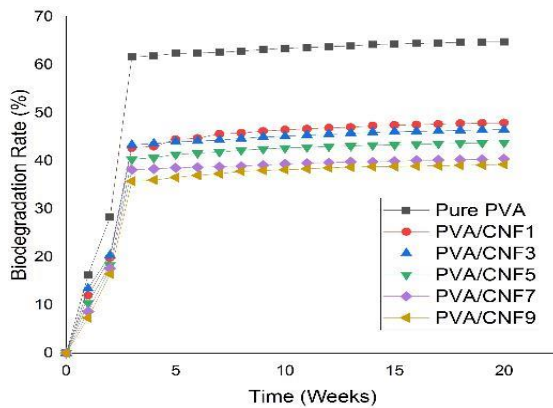
3.5. Biodegradability Test

The rate at which the material can absorb water determines how rapidly it will disintegrate. This process encourages the growth of bacteria and fungicides later on, especially when the material comes into contact with the soil. A soil burial test is often carried out to ascertain a material's biodegradability [24-30]. Soil burial tests were performed on samples of pure PVA, PVA/CMF, and PVA/CNF samples with 1, 3, 5, 7, and 9wt% of filler content, and results were depicted in Figure 13. Almost all the samples exhibited material degradation over a total test period of 20 weeks.

The biodegradability rate of the pure PVA sample was 64.8% at the end of the test period, whereas for PVA/CNF composite with 1, 3, 5, 7, and 9wt% of filler content, BDR was observed to be 47.92%, 46.53%, 43.79%, 40.45%, and 39.25% respectively. Similarly, for PVA/CMF composite with 1, 3, 5, 7, and 9wt% of filler content BDR was observed to be 49.32%, 39.02%, 38.82%, 37.93%, and 33.31% respectively.



a) Pure PVA and PVA/CMF Composites



b) Pure PVA and PVA/CNF Composites

Fig. 13. Biodegradability Rate

From the results obtained, it was evident that the BDR decreased with an increment in filler content. As a result, as the proportion of filler content decreased, the resistance to deterioration decreased, with pure PVA having the lowest resistance to degradation. The decrease in BDR with an increase in filler content was obvious due to the fact that the amount of water uptake decreases at higher filler content which slows down the microbial activity and increases the lifespan of the composite material. A sufficient value of BDR was observed at higher filler contents which indicated that the resulting composites were environmentally friendly and would degrade over a span of time with improved lifespan and performance.

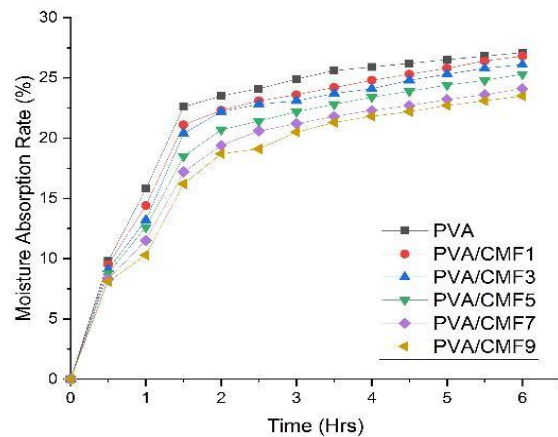
3.6. Moisture Absorption Test

Moisture absorption is one of the most severe issues related to polymeric composite materials which degrades the material's mechanical, thermal, and chemical properties and significantly reduces its performance and lifespan [25-30]. Therefore, in order to ensure the material's predicted performance and lifespan, it is crucial to establish its moisture absorption rate.

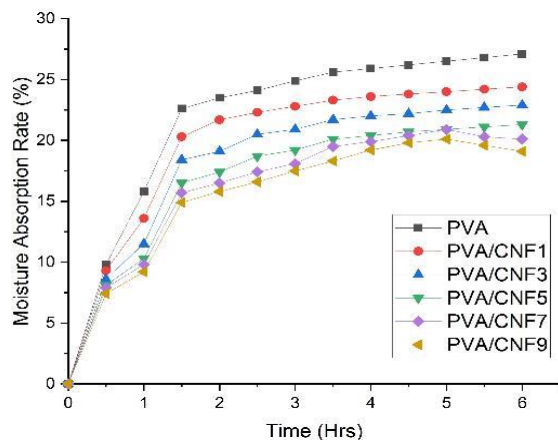
Moisture absorption of pure PVA, PVA/CMF and PVA/CNF composite at 1, 3, 5, 7, and 9wt% of filler content were evaluated and results were depicted in Figure 14. At the end of the test period, the highest moisture absorption rate of 27.1% was seen in pure PVA samples, but it was shown that the rate decreased as the filler proportion increased.

During the first 90 minutes, the moisture absorption rates of all the samples climbed rapidly; however, it was observed that beyond that point, the rate of rise had slowed and was fairly consistent across all of the samples.

After 6 hours of the test period, the moisture absorption rate of PVA/CMF samples with 1, 3, 5, 7, and 9wt% of filler content was observed to be 26.8%, 26.1%, 25.3%, 24.1% and 23.5% respectively and PVA/CNF samples with 1, 3, 5, 7 and 9wt% of filler content exhibited moisture absorption rate of 24.4%, 22.9%, 21.3%, 21.3%, 20.1% and 19.1% respectively. From the results obtained, it can be concluded that the moisture absorption rate decreases with an increase in filler content which will enhance the performance and lifespan of the material.



a) Pure PVA and PVA/CMF Composites



b) Pure PVA and PVA/CNF Composites

Fig. 14. Moisture Absorption Rate

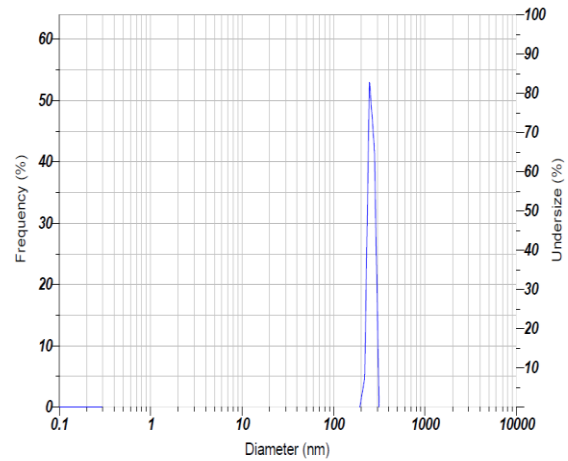
3.7. Particle Size and Zeta Potential Measurement

The distribution of nano cellulose particle sizes is depicted in Figure 15 with a graph that plots frequency in percentage and particle size in percentage versus particle diameter in nm.

The results showed only one intense peak of 83% size having an average particle size being 247.3nm with a mean particle size of 244.0nm and a standard deviation of 16.9nm for CNF, whereas two peaks of intensity 84% and 73% size having average particle size 1595.3 nm with mean particle size of 1218.9 nm and standard deviation of 992.0 nm were observed for CMF. The presence of nano-filler in CNF and micro-filler in CMF in the dispersion demonstrated the efficacy of the mechanochemical treatments used.

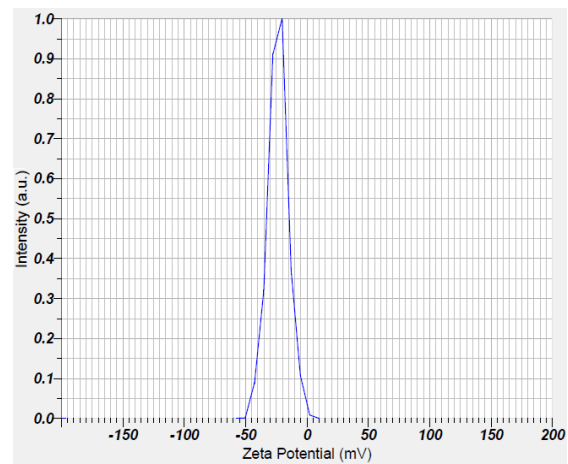
The Zeta potential (ζ) is calculated by measuring particle mobility dispersion in an electric field and is used to determine the stability of a nanocellulose solution in water. The zeta potential of nanocellulose is represented by a graph in Figure 16 which plots intensity in a.u. against zeta potential in mV.

The results showed one peak of intensity 1.0 a.u. for CNF with an average zeta potential being -50 mV with electrophoretic mobility mean of -0.000393 cm²/Vs, while one peak of intensity 1.0 a.u. with an average zeta potential being -23.5 mV with electrophoretic mobility mean of -0.000182cm²/Vs was seen for CMF. The presence of hydroxyl groups accounts for the negative value in both CMF and CNF. As a result of the findings, it is possible to conclude that CNF produced by mechanochemical treatments is electrostatically stable as the absolute value of zeta potential is greater than 25 mV, but CMF produced by chemically treated is electrostatically unstable as the absolute value of zeta potential is less than 25 mV.

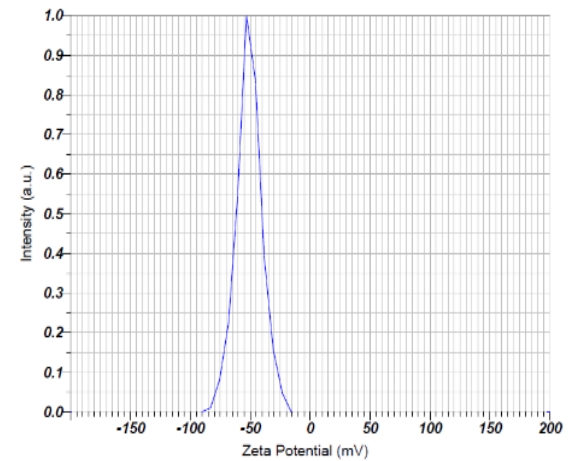


b) Particle size distribution of CNF

Fig. 15. Particle size distribution of CMF and CNF

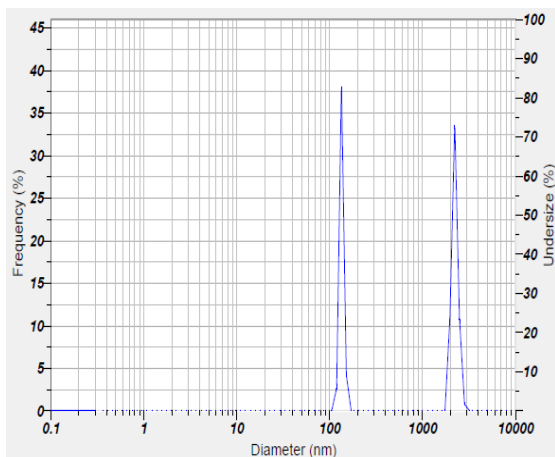


a) Zeta Potential of CMF



b) Zeta Potential of CNF

Fig. 16. Zeta Potential of CMF and CNF



a) Particle size distribution of CMF

4. Conclusions and Future Work

Delonix regia fruit fibers were used in this research work to extract cellulose at micro and nano-scale using mechano-chemical techniques and composite material was prepared using solvent casting method with PVA matrix and extracted cellulose at micro and nano-scale.

Mechanical, thermal, morphological, moisture absorption, and biodegradability of pure PVA, PVA/CMF and PVA/CNF composite at 1, 3, 5, 7, and 9wt% of filler content were evaluated using tensile test, flexural test, impact test, TGA-DTG, SEM and moisture absorption test and soil burial test respectively. Results of SEM indicated that at higher concentrations of filler contents signs of agglomeration started appearing and deteriorated the overall performance of the resulting composite material. For getting uniform distribution of filler content and the optimum performance of composite material filler addition should be restricted below 7wt%.

Results of tensile, flexural, and impact tests showed that nano-fillers exhibited the best performance compared to micro-fillers, and the optimum performance of both composites was obtained below 7wt% filler concentration. TGA and DTG curves indicated that the degradation temperature of composite with filler content improved significantly and composite with nano-fillers had more thermal stability compared to micro-fillers. The results of the biodegradability test and moisture absorption test revealed that the addition of filler content reduced the moisture absorption tendency of the composite and the obtained composite materials had enough biodegradation rate alongwith better lifespan and performance.

Further investigation can be conducted to investigate the effect of plasticizer content on the physical, mechanical, thermal, morphological, and biodegradability properties of the composite material. Also, the bionanocomposite material developed can be utilized for product development and subsequent tests can be conducted on the developed products for feasible applications in aerospace secondary structures.

Acknowledgments

For their assistance and support in material treatment, synthesis, testing, and characterization, I would like to thank the Departments of Physics, Shivaji University, Kolhapur, Department of Metallurgy, National Institute of Technology, Raipur, Tulsiramji Gaikwad-Patil College of Engineering and Technology, Nagpur, Annasaheb Dange College of B. Pharmacy, Sangli and Pt. Ravishankar Shukla University, Raipur.

Conflicts of Interest

The author declares that there is no conflict of interest regarding the publication of this manuscript.

References

- [1] Frone, N., Panaitescu, D. M., Donescu, D., Spataru, C. I., Radovici, C., Trusca, R. and Somoghi, R., 2011. Preparation and characterization of PVA composites with cellulosic nanofibers obtained by ultrasonication. *Bioresources*, 6(1), pp. 487-512.
- [2] Chin, K., Sam, S. T., Ong, H. L., Wong, Y. S., Tan, W. K. and Vannaladsaysy, V., 2022. Bioinspired crosslinked nanocomposites of polyvinyl alcohol-reinforced cellulose nanocrystals extracted from rice straw with ethanedioic acid. *Journal of Nanomaterials*, 3225211, doi: 10.1155/2022/3225211.
- [3] Bahar, E., Ucar, N., Onen, A., Wang, Y., Oksuz, M., Ayaz, O., Ucar, M. and Demir, A., 2012. Thermal and Mechanical Properties of Polypropylene Nanocomposite Materials Reinforced with Cellulose Nano Whiskers. *Journal of Applied Polymer Science*, Vol. 125, pp. 2882–2889, doi: 10.1002/app.36445.
- [4] Fortunati, E., Puglia, D., Monti, M., Santulli, C., Maniruzzaman, M. and Kenny, J. M., 2012. Cellulose Nanocrystals Extracted from Okra Fibers in PVA Nanocomposites. *J. Appl. Polym. Sci.*, doi: 10.1002/app.38524.
- [5] Niazi, M. B. K., Jahan, Z., Berg, S. S. and Gregersen, O. W., 2017. Mechanical, thermal and swelling properties of phosphorylated nanocellulose fibrils/PVA nanocomposite membranes. *Carbohydrate Polymers*, doi: 10.1016/j.carbpol.2017.08.125.
- [6] Kaurase, K. P. and Singh, D., 2020. Delonix Regia Fruit Fibers: A new potential source of cellulosic fibers. Materials Science Forum, *Trans Tech Publications Ltd*, 979, pp. 185-196, doi: 10.4028/www.scientific.net/MSF.979.185.
- [7] Perumal, B., Sellamuthu, P. S., Nambiar, R. B. and Sadiku, E. R., 2018. Development of polyvinyl alcohol/ chitosan bio-nanocomposite films reinforced with cellulose nanocrystals isolated from rice straw. *Appl. Surf. Sci.*, doi: 10.1016/j.apsusc.2018.01.022.
- [8] Fortunati, E., Puglia, D., Luzi, F., Santulli, C., Kenny, J. M. and Torre, L., 2013. Binary PVA bio-nanocomposites containing cellulose nanocrystals extracted from different natural sources: Part I, *Carbohydrate Polymers*. doi: 10.1016/j.carbpol.2013.03.075.

- [9] Kaurase, K. P. and Singh, D., 2020. Investigation on Chemical Isolation and Characterization of Cellulose from Delonix regia Fruit Fibers. In: Vijayan S., Subramanian N., Sankaranarayananasamy K. (eds) *Trends in Manufacturing and Engineering Management, Lecture Notes in Mechanical Engineering*, pp. 303-314, doi: 10.1007/978-981-15-4745-4_28.
- [10] Kaurase, K. P. and Singh, D., 2022. Isolation of Cellulosic Nano Fibers from Delonix Regia Fruits by Mechano-chemical Route. *International Journal of Vehicle Structures and Systems*, 14(4), pp. 518-523, doi: 10.4273/ijvss.14.4.19.
- [11] Rescignano, N., Fortunati, E., Montesano, S., Emiliani, C., Kenny, J. M., Martino, S. and Armentano, I., 2013. PVA bio-nanocomposites: a new take-off using cellulose nanocrystals and PLGA nanoparticles. *Carbohydrate Polymers*, doi: 10.1016/j.carbpol.2013.08.061.
- [12] Pereira, L. S., Nascimento, D. M., Filho, M. M. S., Morais, J. P. S., Vasconcelos, N. F., Feitosa, J. P. A., Brigida, A. I. S. and Rosa, M. F., 2014. Improvement of polyvinyl alcohol properties by adding nanocrystalline cellulose isolated from banana pseudostems. *Carbohydrate Polymers*, doi: 10.1016/j.carbpol.2014.05.090.
- [13] Liu, D., Sun, X., Tian, H., Maiti, S. and Ma, Z., 2013. Effects of cellulose nanofibrils on the structure and properties on PVA nanocomposites. *Cellulose*, 20, pp. 2981-2989, doi: 10.1007/s10570-013-0073-6.
- [14] Bondeson, D. and Oksman, K., 2007. Polylactic acid/cellulose whisker nanocomposites modified by polyvinyl alcohol. *Composites: Part A*, 38, pp. 2486-2492, doi: 10.1016/j.compositesa.2007.08.001.
- [15] Kassab, Z., Boujemaoui, A., Youcef, H. B., Hajlane, A., Hannache, H. and Achaby, M. E., 2019. Production of cellulose nanofibrils from alfa fibers and its nanoreinforcement potential in polymer nanocomposites. *Cellulose*, doi: 10.1007/s10570-019-02767-5.
- [16] Chaabouni, O. and Boufi, S., 2017. Cellulose nanofibrils/polyvinyl acetate nanocomposite adhesives with improved mechanical properties. *Carbohydrate Polymers*, 156, pp. 64-70, doi: 10.1016/j.carbpol.2016.09.016.
- [17] Spagnol, C., Fragal, E. H., Witt, M. A., Follmann, H. D. M., Silva, R. and Rubira, A. F., 2018. Mechanically improved polyvinyl alcohol-composite films using modified cellulose nanowhiskers as nanoreinforcement. *Carbohydrate Polymers*, doi: 10.1016/j.carbpol.2018.03.001.
- [18] Ali, M. A. S. S., Jimat, D. N., Nawawi, W. M. F. W. and Sulaiman, S., 2021. Antibacterial, Mechanical and Thermal Properties of PVA/Starch Composite Film Reinforced with Cellulose Nanofiber of Sugarcane Bagasse. *Arabian Journal for Science and Engineering*, doi: 10.1007/s13369-021-05336-w.
- [19] Jahan, Z., Niazi, M. B. K. and Gregersen, O. W., 2017. Mechanical, thermal and swelling properties of Cellulose Nanocrystals/PVA nanocomposites membranes. *Journal of Industrial and Engineering, Chemistry*, doi: 10.1016/j.jiec.2017.08.014.
- [20] Meesorn, W., Shirole, A., Vanhecke, D., Espinosa, L. M. and Weder, C., A Simple and Versatile Strategy To Improve the Mechanical Properties of Polymer Nanocomposites with Cellulose Nanocrystals, *Macromolecules*, 2016, doi: 10.1021/acs.macromol.6b02629.
- [21] Chen, H. Z. Li, S. C. and Wang, Y. Z., 2015. Preparation and characterization of nanocomposites of polyvinyl alcohol/cellulose nanowhiskers/chitosan. *Composites Science and Technology*, doi: 10.1016/j.compscitech.2015.05.004.
- [22] Yang, M., Zhang, X., Guan, S., Dou, Y. and Gao, X., 2020. Preparation of lignin containing cellulose nanofibers and its application in PVA nanocomposite films. *International Journal of Biological Macromolecules*, doi: 10.1016/j.ijbiomac.2020.05.044.
- [23] Kassab, Z., Mansouri, S., Tamraoui, Y., Sehaqui, H., Hannache, H., Qaiss, A. E. K. and Achaby, M. E., 2020. Identifying Juncus plant as viable source for the production of micro- and nano-cellulose fibers: Application for PVA composite materials development. *Industrial Crops & Products*, 144, 112035, doi: 10.1016/j.indcrop.2019.112035.
- [24] Alamri, H. and Low, I. M., 2012. Effect of water absorption on the mechanical properties of n-SiC filled recycled cellulose fibre reinforced epoxy eco-nanocomposites. *Polymer Testing*, 31, pp. 810-818, doi: 10.1016/j.polymertesting.2012.06.001.

- [25] Irvin, W., Satam, C. C., Meredith, J. C. and Shofner, M. L., 2018. Mechanical Reinforcement and Thermal Properties of PVA Tricomponent Nanocomposites with Chitin Nanofibers and Cellulose Nanocrystal. *Composites: Part A*, doi: 10.1016/j.compositesa.2018.10.028.
- [26] Kaboorani, A., Riedl, B., Blanchet, P., Fellin, M., Hosseinaei, O. and Wang, S., 2012. Nanocrystalline cellulose (NCC): A renewable nano-material for polyvinyl acetate (PVA) adhesive. *European Polymer Journal*, 48, pp. 1829-1837, doi: 10.1016/j.eurpolymj.2012.08.008.
- [27] Sanjeevi, S., Shanmugam, V., Kumar, S., Ganesan, V., Sas, G., Johnson, D. J., Shanmugam, M., Ayyanar, A., Naresh, K., Neisiany, R. E. and Das, O., 2021. Effects of water absorption on the mechanical properties of hybrid natural fibre/phenol formaldehyde composites. *Scientific Reports*, 11, 13385, doi: 10.1038/s41598-021-92457-9.
- [28] Millon, L. E., Oates, C. J. and Wan, W., 2009. Compression Properties of Polyvinyl Alcohol-Bacterial Cellulose Nanocomposite. *J Biomed Mater Res Part B, Appl Biomater* 90B, pp. 922-929, doi: 10.1002/jbm.b.31364.
- [29] Rafieian, F., Shahedi, M., Keramat, J. and Simonsen, J., 2014. Mechanical, thermal and barrier properties of nano-biocomposite based on gluten and carboxylated cellulose nanocrystals. *Industrial Crops and Products*, 53, pp. 282-288, doi: 10.1016/j.indcrop.2013.12.016.
- [30] Alamri, H. and Low, I. M., 2012. Effect of water absorption on the mechanical properties of nano-filler reinforced epoxy nanocomposites. *Materials and Design*, 42, pp. 214-222, doi: 10.1016/j.matdes.2012.05.060.
- [31] Rana, S. S. and Gupta, M. K., 2021. Variations in the mechanical properties of bionanocomposites by water absorption. *J Materials: Design and Applications*.
- [32] Razzaq, W., Javaid, A., 2015. Synthesis & Characterization of cotton fiber reinforced starch/PVA biodegradable composite films. *Journal of Faculty of Engineering & Technology*, 22(1).
- [33] Danni, N., Sasikumar, T. and Fazil, A. A., 2016. Mechanical Properties of Electrospun CNF/PVA Nanofiber Mats as Reinforcement in Polymer Matrix Composites. *International Journal of Applied Chemistry*, 12(2), pp. 107-119.
- [34] Shafiq, N., Ayub, T. and Khan, S. U., 2016. Investigating the performance of PVA and basalt fibre reinforced beams subjected to flexural action. *Composite Structures*, 153, pp. 30-41, doi: 10.1016/j.compstruct.2016.06.008.
- [35] Pandey, S., Pandey, S. K., Parashar, V., Mehrotra, G. K. and Pandey, A. C., 2011. Ag/PVA nanocomposites: optical and thermal dimensions. *J. Mater. Chem.*, 21, pp. 17154-17159.
- [36] Stepanova, M. and Vlakh, E. K., 2022. Modification of Cellulose Micro- and Nanomaterials to Improve Properties of Aliphatic Polyesters/Cellulose. *Composites: A Review, Polymers*, 14, 1477, doi: 10.3390/polym14071477.
- [37] Kumar, T. S. M., Rajini, N., Jawaid, M., Rajulu, A. V. and Jappes, J. T. W., 2017. Preparation and Properties of Cellulose/Tamarind Nut Powder Green Composites. *Journal of Natural Fibers*, doi: 10.1080/15440478.2017.1302386.
- [38] Lamaming, J., Hashim, R., Leh, C. P., Sulaiman, O. and Lamaming, S. Z., 2020. Bio-nanocomposite Films Reinforced with Various Types of Cellulose Nanocrystals Isolated from Oil Palm Biomass Waste. *Waste and Biomass Valorization*, 11, pp. 7017-7027, doi: 10.1007/s12649-019-00892-7.
- [39] Rana, R. S., Rana, S., Nigrawal, A., Kumar, B. and Kumar, A., 2020. Preparation and mechanical properties evaluation of polyvinyl alcohol and banana fibres composite. *Materials Today: Proceedings*, doi: 10.1016/j.matpr.2020.02.648.
- [40] Kakroodi, R., Cheng, S., Sain, M. and Asiri, A., 2014. Mechanical, Thermal, and Morphological Properties of Nanocomposites Based on Polyvinyl Alcohol and Cellulose Nanofiber from Aloe Vera Rind. *Journal of Nanomaterials*, 903498, doi: 10.1155/2014/903498.
- [41] Bacha, G., Demsash, H. D., Shumi, L. D. and Debesa, B. E., 2022. Investigation on Reinforcement Effects of Nanocellulose on the Mechanical Properties, Water Absorption Capacity, Biodegradability, Optical Properties, and Thermal Stability of a Polyvinyl Alcohol Nanocomposite Film. *Advances in Polymer Technology*, 6947591, doi: 10.1155/2022/6947591.

- [42] Silverio, H. A., Neto, W. P. F., Silva, I. S. V., Rosa, J. R., Pasquini, D., Assunção, R. M. N., Barud, H. S. and Ribeiro, S. J. L., 2014. Mechanical, Thermal and Barrier Properties of Methylcellulose/Cellulose Nanocrystals Nanocomposites. *Polimeros*, 24(6), pp. 683-688, doi: 10.1590/0104-1428.1691.
- [43] Niazi, M. B. K., Jahan, Z., Ahmed, A., Uzair, B., Mukhtar, A. and Gregersen, O. W., 2020. Mechanical and Thermal Properties of Carboxymethyl fibers (CMF)/PVA based nanocomposite membranes. *Journal of Industrial and Engineering Chemistry*, doi: 10.1016/j.jiec.2020.07.004.
- [44] Kaurase, K. P. and Singh, D., 2023. Mechanical and Barrier Properties of Cellulosic Nano-Fibers Reinforced Bionanocomposite. *International Journal of Vehicle Structures and Systems*, 15(1), pp. 46-51, doi: 10.4273/ijvss.15.1.08.